IV International Conference on Particle-based Methods – Fundamentals and Applications
PARTICLES 2015
E. Oñate, M. Bischoff, D.R.J. Owen, P. Wriggers & T. Zohdi (Eds)

INVESTIGATION OF TIRE-SOIL-INTERACTIONS USING THE DISCRETE-ELEMENT-METHOD

OLIVER ZIEHER[1] AND MARTIN MEYWERK[2]

[1] Helmut-Schmidt-Universität
Holstenhofweg 85
22043 Hamburg
Germany
Oliver.Zieher@hsu-hh.de

[2] Helmut-Schmidt-Universität
Holstenhofweg 85
22043 Hamburg
Germany
Martin.Meywerk@hsu-hh.de

Key words: Granular Materials, Discrete Element Method, Soft Soil, Tyre-Soil-Interaction

Abstract. In this article a tyre is investigated which moves in lateral direction, i.e. perpendicular to its regular rolling direction, through sand, which is one representative of a deformable soil. This kind of motion could be a result of skidding of a car where the vehicle slides laterally over the side verge. In order to investigate this motion in the first step the influence of the compliance of the tyre is studied; the result is that an flexible tyre behaves similar to an rigid one. Therefore, in the second step, the simulations and the experimental investigations of the tyre are restricted to a stiff tyre, the results of experiments and simulations with an discrete element method are compared, the influence of some parameters are studied.

1 INTRODUCTION

Different analytical approaches for tyre-soil-interaction are described in literature. Mostly this approaches are used to predict the traction behaviour and the wheel-soil rolling resistance. Extensions of this approaches are capable to predict lateral behaviour and lateral forces during rolling motion with a non-zero slip angle [3].

Often the vertical behaviour of the soil is described by the theory of Bekker [5], whereas the tangential effects are predicted by the approach of Janosi und Hanamoto [4]. In order to describe more complicated cases, where a multi-axial state of stress is important, the Finite Element Method (FEM) can be used. FEM is limited in the case of large deformations or in the case of disruptions. For large deformations and disruptions a

particle method is appropriate, especially in case of non cohesive soils like sand. Therefore, the soil-tyre-interactions we consider in this article is simulated with a particle method, the so-called discrete element method (DEM). In [1, 6] similar situations are simulated with the discrete element method, where plates moving through granular materials. A overview about existing tire-terrain models you can find in [7].

2 EXPERIMENTAL SETUP

For the experimental investigations of the tyre-soil-interaction a modified crash sled test facility is used (cf. Fig. 1(b)). The principal test setup is shown in Fig. 2. The sled 1 with rollers runs on the guide rails ⑤. The guidance ensures only one longitudinal degree of freedom of the sled. The mass of the sled without additional components is 854 kg. On each side of the sled a lever arm ② is mounted with a revolute joint to the sled. The left and the right lever arms are connected by a beam ⑥. The mass of the lever arms and the beam is 702 kg. At one end of each lever arm a wheel (195/65 R15) is mounted. The two wheels interact with sand in two trough fixed on the floor on the right and the left side. That means, that the whole setup is symmetric and nearly no moments with respect to the vertical axis and no lateral forces are acting on the sled. This is an important restriction of the whole construction, because the sled and the guide rails are not designed for large loads of the mentioned kind. The dimensions of the two troughs are: length l=4000 mm, width w=800 mm, height h=400 mm.

The sled is accelerated by several bungee ropes. During acceleration the lever arms are locked by an electromagnet in a horizontal position. Immediately after the wheels are complete over the sand trough at their beginning, the electromagnet is deactivated and the lever arms together with the wheels are accelerated by gravitation. The result is, that the wheels come into contact with the sand and sink into the sand (cf. Fig. 1(a)).

(a) (b)

Figure 1: Interaction between wheel and sand (a) and experimental setup (b)

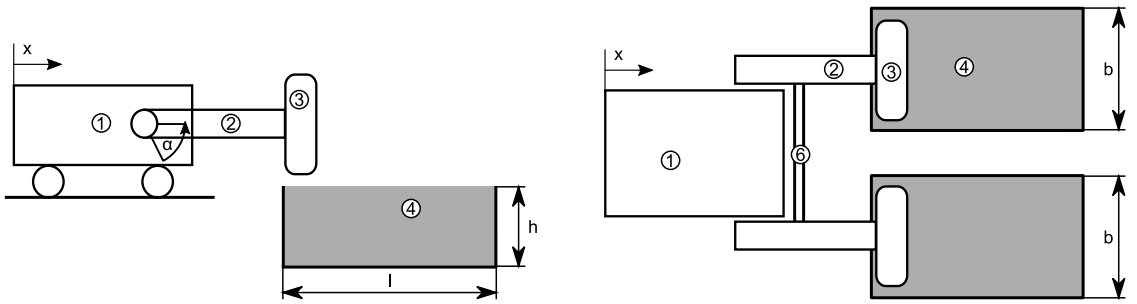

(a) side view (b) top view

Figure 2: Principal drawing of the experimental setup

3 INFLUENCE OF THE TYRE COMPLIANCE

In a first step the influence of the tyre compliance is experimentally investigated. This is an important aspect for the simulation, because a tyre, which could be assumed rigid in the particle simulation, is easier and needs less resources.

To obtain a comparison between stiff and deformable tyres, the results of two experimental setups are compared: In the first setup an deformable tyre is used, in the second one a stiff surrogate tyre made out of aluminium and polyoxymethylene (cf. Fig. 3). The outer contours of both, deformable and stiff tyre are similar, the tyre patterns are neglected in the surrogate tyre. To obtain similar friction behaviour, the surface of the surrogate tyre is bonded with abrasive paper. Furthermore, the surrogate tyre is completed with an additional mass to obtain the same mass of the tyres.

It is known that the mechanical behaviour of soils depends on the consolidation. Therefore, the sand in the troughs is consolidated by a plate vibrator. This ensures small variations in the experimental results.

To compare the two types of tyre objects (stiff and deformable) we look at the sinkage $h = h(s)$ and the velocity $v = v(s)$ in dependence of the displacement s of the sled. The value $s = 0m$ is equivalent to that point in time where the arm is horizontal. The sinkage which corresponds of first contact between tyre and sand is between nearly zero sinkage $h = 0$ mm and approximately $h = 10$ mm; the sinkage of first contact depends on the consolidation treatment of the sand. The sinkage h is depicted in Fig. 4(a) for two experiments with a stiff tyre and one with a deformable one. The initial velocities differ slightly in the experiments (cf. Fig. 4(b)). It is obvoius, that the sinkage up to a displacement of $s \approx 0.4$ m for both tyre objects are nearly the same, differences are the result of differences in the initial velocities, the different tyre types and differences in the characteritics of the soil. Variations in the characteristics of the soil, this means variations between different experiments and spatial variations within the troughs are one of the most challenging aspects in order to obtain reliable experimental results. Oscillations occur in the deformable tyre experiments, whereas no such oscillations can be seen in the stiff tyre experiments.

This experiments show that there are small differences between a stiff and a deformable tyre. This is the reason, that for the characterisation and the simulation of sand with DEM it is sufficient to take the stiff tyre experiments.

Figure 3: Deformable tyre and stiff surrogate tyre

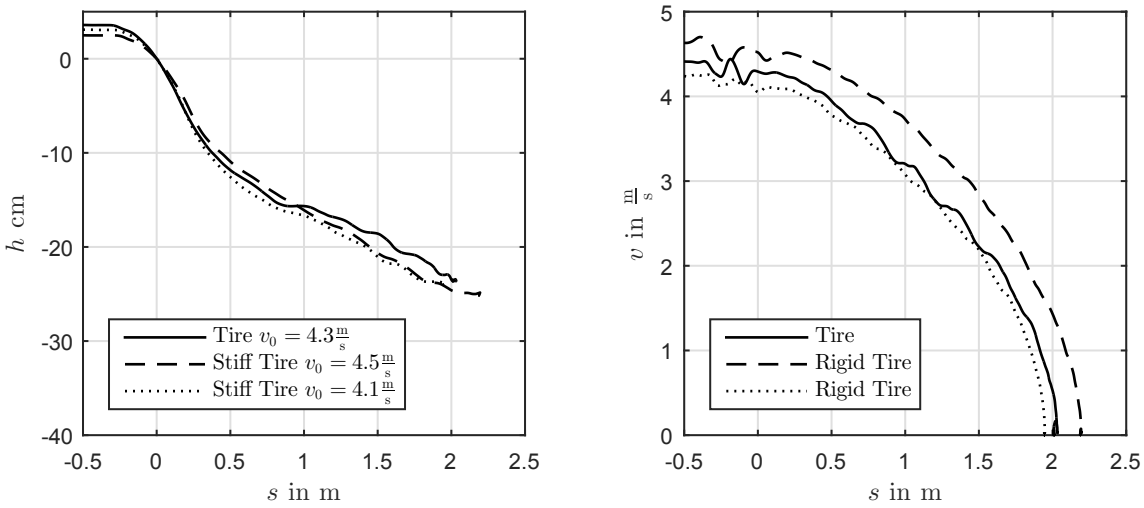

(a) (b)

Figure 4: Comparison of two Measurements of a flexible tire and the stiff surrogate tyre

4 SIMULATION

4.1 DEM

One common method to simulate granular media, e.g., sand, is the DEM, particular if the dynamical behaviour including inertia effects are important. In this article the open

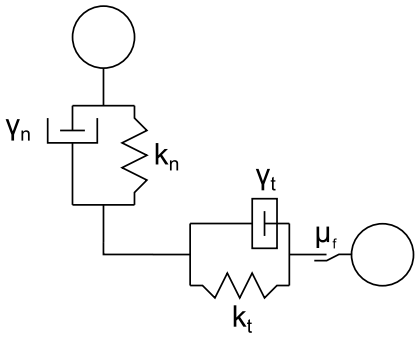

Figure 5: Interaction model of two elements

source software LIGGGHTS is used; the equations of this section are from the user manual of LIGGGHTS. The forces between the elements are calculated by force displacement relations which are illustrated in Fig. 5. The stiffness and damping parameters are given implicitely, for example by Youngs's modulus.

For example the normal contact stiffness

$$k_n = \frac{4}{3} Y^* \sqrt{R^* \delta_n} \tag{1}$$

is dependent on a equivalent Young's modulus Y^*, an equivalent radius R^* of the elements and the penetration δ_n. The parameters Y^* and R^* can be calculated similar to Hertz's contact theory from Youngs's moduli Y_1, Y_2, Poisson's ratios ν_1, ν_2 and the radii R_1, R_2, of the two bodies in contact:

$$\frac{1}{Y^*} = \frac{(1-\nu_1^2)}{Y_1} + \frac{(1-\nu_2^2)}{Y_2} \tag{2}$$

and

$$\frac{1}{R^*} = \frac{1}{R_1} + \frac{1}{R_2} \ . \tag{3}$$

The tangential stiffness can calculated by

$$k_t = 8 G^* \sqrt{R^* \delta_n} \tag{4}$$

using an equivalent shear modulus

$$\frac{1}{G^*} = \frac{2(2+\nu_1)(1-\nu_1)}{Y_1} + \frac{2(2+\nu_2)(1-\nu_2)}{Y_2}. \tag{5}$$

The coefficients of damping in normal and tangential direction γ_n and γ_t, resp., can be calculated using the coefficient of restitution β

$$\gamma_n = -2\sqrt{\frac{5}{6}}\ \beta \sqrt{S_n m^*} \geq 0 \tag{6}$$

where

$$S_n = 2Y^* \sqrt{R^* \delta_n} \tag{7}$$

and

$$\gamma_n = -2\sqrt{\frac{5}{6}}\, \beta \sqrt{S_t m^*} \geq 0 \ ; \tag{8}$$

here

$$S_t = 8G^* \sqrt{R^* \delta_n} \ . \tag{9}$$

Furthermore, it is possible that torques are acting between the grains, which can be included by friction torques

$$\overrightarrow{M_{rf}} = \mu_{roll} k_n \delta_n \frac{\overrightarrow{\omega_{r,scher}}}{|\overrightarrow{\omega_{r,scher}}|} R^* \ . \tag{10}$$

Here, μ_{roll} is a coefficient of rolling resistance, $\overrightarrow{\omega_{r,scher}}$ is the projection of $\overrightarrow{\omega_r}$ onto the plane, which is tangential to both elements in the point of contact. The vector of the angular velocity $\overrightarrow{\omega_r}$ is the result of the vectors of angular velocities of the two interacting elements.

4.2 Generating the porosity

The porosity η is defined by

$$\eta = \frac{V_v}{V} \tag{11}$$

where V_v is the volume of the voids and V is the total volume of the bulk material.

In the experiments carried out the values of the porosity differ from 0.35 (consolidated) to 0.50 (loose). Therefore, it is essential to adjust the porosity in the simulation, too. To achieve certain values of the porosity the following procedure is applied: In the first step the positions of the elements are generated randomly one by one. If a new element intersects with an already existing one, this new element is refused by the algorithm and a new randomly generated particle is placed (this random generation is repeated until the new element has no intersection to an existing one). With this first step porosities $\eta > 0.7$ can be generated. To reach the goal of smaller porosities $\eta_t \leq 0.7$ a second step is necessary in which the element distribution generated in the first step wit $\eta_0 > 0.7$ is modified by increasing the diameters of all particles during a simulation with full consideration of contact conditions and movement of the particles. If an increase factor of

$$\zeta = \sqrt[3]{\frac{1-\eta_0}{1-\eta_t}} \tag{12}$$

is reached, the final porosity is η_t.

4.3 Parametrisation

A direct experimental determination of the DEM parameters is not possible (cf. [2]). Therefore, different experiments are used in a parameter identification process, in which the experiments are simulated and the parameters are optimized in order to obtain similar simulation results compared to the experimental results.

The coefficient of friction μ_f is measured in a shear tester, which consists of an upper and a lower box (cf. Fig. 6(a)). The sand in the box is loaded by a normal force F_n. Then the lower box is moved horizontal with a low shear velocity of $v_s \approx 0.08\frac{\mathrm{m}}{\mathrm{s}}$. The shear force F_s is measured at the upper box. This experimental setup allows the determination of a coefficient of friction μ_f by simulating the shear test. The result is $\mu_f = 0.8$ for the sand investigated in this paper.

A so-called oedometer allows the determination of the Youngs's modulus. Fig. 6(b) shows a principal sketch of the experimental setup. Since the box is closed in both horizontal directions the vertical load results in a vertical displacement of the load plate, the lateral strain is zero. This experiments yields a Youngs's modulus of 500 MPa.

The determination of the coefficient μ_{roll} of rolling resistance is possible by investigating experimentally the angle of repose.The angle of repose is the maximum angle between the shoulder of a cone-shaped pile of the sand and the horizontal, where the cone-shaped pile is generated with out slumping of the sand. Fig. 7 shows the pile for the sand used in this investigation (Test) in the background. In the foreground the simulation results of the pile are shown for different values of the coefficient μ_{roll}. For $\mu_{roll} = 0.3$ the experimental pile and the simulated one corresponds good to each other.

The influence of the coefficient of restitution β and Poisson's ratio ν are small, values for β and ν are comprised in Table 1.

Table 1: Simulation Parameters

Description	Symbol	Value	Unit
Young's modulus	Y	500	MPa
Poissons ratio	ν	0.3	-
Coefficient restitution	β	0.3	-
Coefficient of friction	μ_f	0.8	-
Coefficient of rolling friction	μ_{roll}	0.3	-
Element density	ρ	2700	$\frac{\mathrm{m}}{\mathrm{s}}$
Element radius	R	6	mm

4.4 Comparison of experimental results and simulation

The parameters of the DEM are chosen as described in the previous section. The porosity η is a crucial parameter for a good agreement between experimental result and

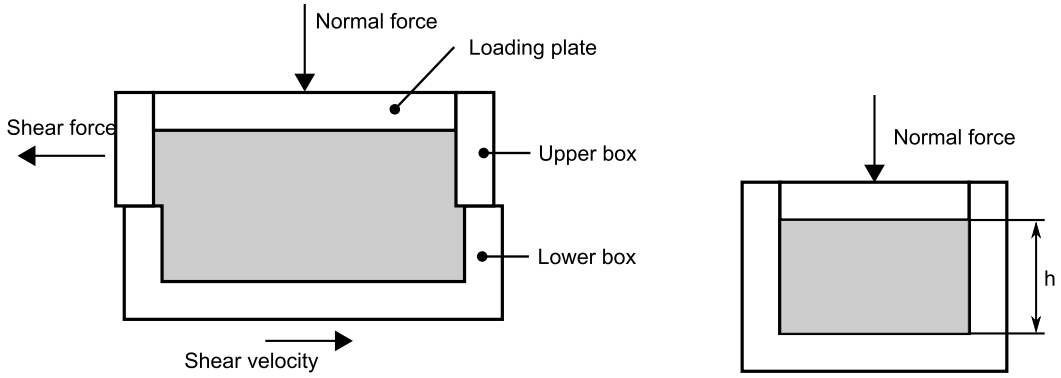

Figure 6: Sketch of the Direct Shear Tester(a) and compression testing device(b)

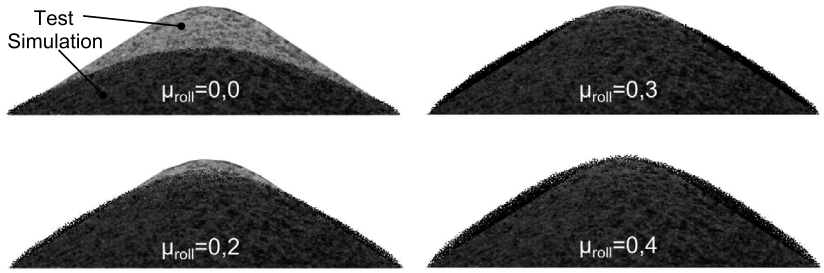

Figure 7: Comparison between a picture of a sand pile an the result of a simulation with different coefficient of rolling friction

simulation, furthermore, the results are highly sensitive on this parameter. The porosity depends strongly on the consolidation of the sand in the trough. Unfortunately, it is very expensive to determine η in the sand. This is the reason for fitting η in order to obtain good agreement between experiments and simulation. Doing this, the sinkage-displacement-function $h(s)$ of the tyre and the velocity-displacement-function $v(s)$ of the sled of the experiment and the simulation is used.

Fig. 8 shows a comparison of $h(s)$ and $v(s)$ for a highly consolidated sand of a porosity of $\eta = 0.59$. A good agreement between the experiments and the simulation is obvious.

More results are shown in Fig. 9 for not highly consolidated sand, the porosity is $\eta = 0.405$. Whereas the agreement of the velocity $v(s)$ is better for $\eta = 0.405$ as for $\eta = 0.59$ shown in 8, the agreement of the sinkage s is better for $\eta = 0.59$ shown in 8.

4.5 Simulations using optimized parameters

Further investigations and comparisons between experiments and simulations show that the agreement can be improved. If the coefficient μ_{roll} of rolling resistance is increased compared to the value which is determined using the experiment for determination of the

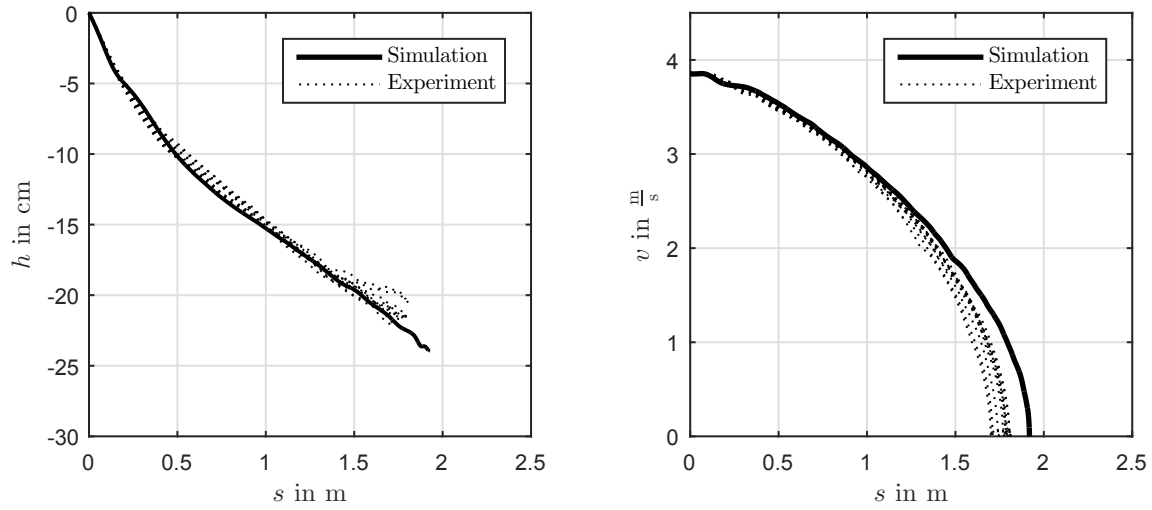

(a) (b)

Figure 8: Comparison of experiment and a simulation with a porosity η of 0.59, which is fitted by the sinkage-displacement-function

angle of repose, then a better agreement can be achieved. For an increased value of μ_{roll} the sinkage decreases, which is compensated by an increased porosity. Fig. 10 shows the comparison for $\mu_{roll} = 0.6$ and $\eta = 0.4175$ and good agreement between experiments and simulation.

5 CONCLUSION

It is shown that it is possible to obtain a good agreement between experiments and simulation for the sled test with the rigid tyre. Furthermore, the generation of a specific porosity for the DEM is shown. Optimized parameters which differ from those advised by the simple experiment of the angle of repose are recommended.

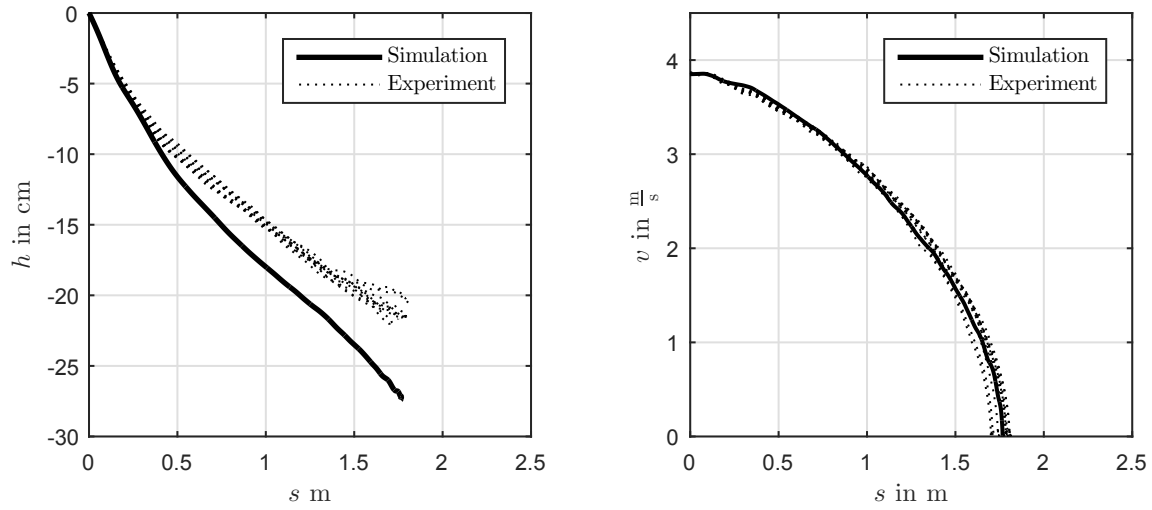

(a) (b)

Figure 9: Comparison of experiment and a simulation with a porosity η of 0.405, Which is fitted by the velocity-displacement-function

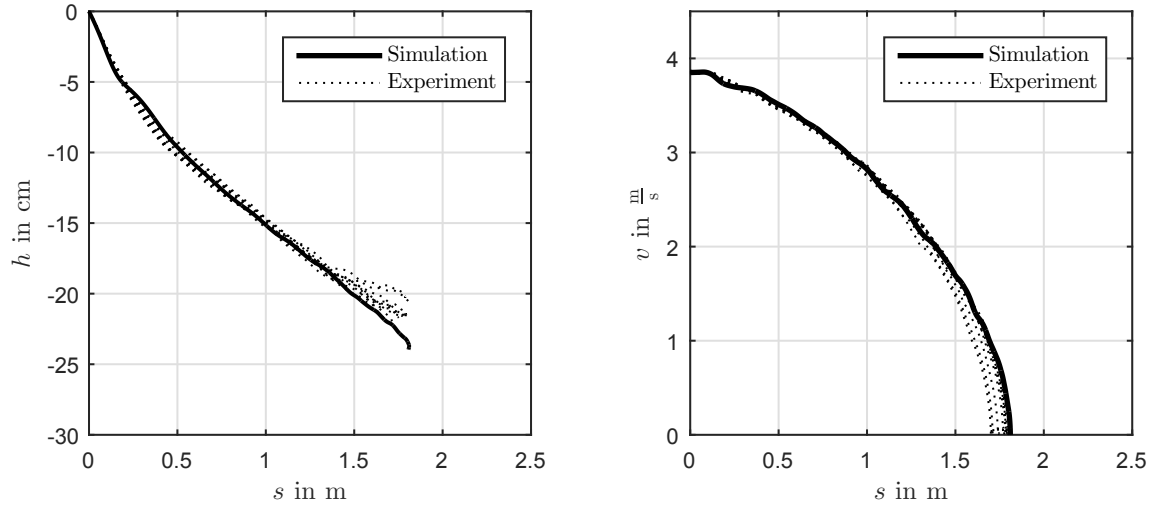

(a) (b)

Figure 10: Comparison of experiment and a simulation with optimized parameters: η=0.4175 and μ_{roll}=0,60

REFERENCES

[1] Obermayr, M., Dressler ,K., Vrettos ,C. and Eberhard ,P., Prediction of draft forces in cohesionless soil with the Discrete Element Method *Journal Of Terramechanics* (2011) **48**:347–358.

[2] Huang, Y., Three dimensional simulation of lunar dust levitation under the effect of simulated sphere body *Journal of Terramechanics* (2011) **48**:297–306.

[3] Harnisch, C., *Dynamische Echtzeitsimulation der Gelndefahrt mehrachsiger Radfahrzeuge* (2001)

[4] Janosi, Z. and Hanamoto, B., The analytical determination of drawbar pull as a function of slip for tracked vehicles in deformable soils. *First international Conference on Soil Mechanics of Soil-Vehicle Systemst* (1961)

[5] Bekker, M. G., Introduction to Terrain-Vehicle Systems. *The University of Michigan Press* (1961)

[6] Tsuji, T., Nakagawa Y., Matsumoto, N., Kadono, Y., Takayama, T., Tanaka, T., 3-D DEM simulation of cohesive soil-pushing behavior by bulldozer blade *Journal of Terramechanics* (2012) **49**:37–47.

[7] Taheri, Sh., Sandu, C., Taheri, S., Pinto, E. and Gorisch, D., A technical survey on Terramechanics models for tire-terrain interaction used in modeling and simulation of wheeled vehicles *Journal of Terramechanics* (2015) **57**:1–22.